

Classification and Mapping of Fuels in Mediterranean Forest Landscapes Using a UAV-LiDAR System and Integration Possibilities with Handheld Mobile Laser Scanner Systems

Raúl Hoffrén ^{1,2}, María Teresa Lamelas ^{2,3,*} and Juan de la Riva ^{1,2}

- ¹ Department of Geography and Land Management, University of Zaragoza, Calle Pedro Cerbuna 12, 50009 Zaragoza, Spain; rhoffren@unizar.es (R.H.); delariva@unizar.es (J.d.l.R.)
- ² Geoforest Group, University Institute for Research in Environmental Sciences of Aragón (IUCA), University of Zaragoza, Calle Pedro Cerbuna 12, 50009 Zaragoza, Spain
- ³ Centro Universitario de la Defensa, Academia General Militar, Ctra. Huesca s/n, 50090 Zaragoza, Spain
- * Correspondence: tlamelas@unizar.es

Table S1. Description and general characteristics of the forest plots. XY coordinates in ETRS89 / UTM zone 30N (EPSG: 25830).

Sector	Plot name	FT	X	Y	UAV points/m ² density	HMLS points/m ² density
Almudévar	al01	5	694602.4	4652067.8	562.11	71,594.08
	al02	5	694567.6	4652104.5	562.11	61,510.30
	al03	4	710134.0	4663293.6	502.80	55,084.31
	al04	4	710141.3	4663668.7	502.80	55,983.11
	al05	5	697105.5	4653417.9	457.56	-
	al06	5	697077.0	4653418.3	457.56	-
	al07	5	697017.0	4653403.3	457.56	-
	al08	5	697328.8	4653490.1	457.56	91,474.10
	al09	5	697275.2	4653516.2	457.56	69,930.07
Ayerbe	ay01	7	687724.6	4676577.7	548.62	-
	ay02	7	686539.2	4676302.0	527.17	-
	ay03	6	686345.4	4676281.1	527.17	-
	ay04	6	686687.0	4674577.9	549.93	133,259.23
	ay05	7	686571.7	4674322.0	484.65	-
	ay06	6	688450.4	4674202.7	408.93	89,334.00
	ay07	7	686360.6	4674755.4	402.53	-
	ay08	6	686536.4	4674651.8	549.93	84,663.50
	ay09	7	686777.5	4674151.0	484.65	-
	ay10	7	686827.2	4674370.8	336.32	-
	ay11	7	687030.2	4674287.7	336.32	-
	ay12	5	685055.4	4672393.5	487.08	29,699.16
	ay13	7	688074.2	4673849.8	443.70	-
	ay14	6	688185.8	4673837.0	443.70	-
	ay15	6	688256.4	4674080.0	408.93	80,750.19
	ay16	7	688792.3	4674281.6	506.80	115,322.61
	ay17	7	689248.8	4674261.2	406.49	131,697.66
	ay18	7	689238.5	4674206.1	406.49	-
	ay19	6	686878.8	4673256.3	459.62	119,540.63
	ay20	6	686703.7	4673179.9	459.62	84,514.25
	ay21	6	686995.7	4672946.4	311.16	-
	ay22	7	687240.4	4673227.3	351.69	77,658.80
	ay28	6	688371.2	4673218.0	489.35	82,040.58
	ay29	7	688737.6	4673129.7	426.31	85,566.76
	ay30	7	688775.1	4673342.4	292.70	78,094.99
	ay31	7	688609.8	4673178.1	426.31	78,879.46
	ay44	7	686251.9	4671350.2	457.55	-
	ay45	7	686273.1	4671283.0	457.55	-
	ay46	6	686986.9	4671460.5	453.52	-
	ay47	5	685130.0	4673135.5	644.98	31,830.43
	ay48	5	685134.6	4673047.1	644.98	-
	ay49	5	685076.3	4672599.0	487.08	52,189.62
	ay50	5	685122.5	4672511.9	487.08	24,966.82
Uncastillo	un02	5	643660.3	4693452.8	232.77	-
	un03	6	643147.3	4693675.1	330.96	-
	un04	3	643639.7	4694117.3	394.52	-
	un05	7	652269.5	4700453.3	306.03	-
	un11	3	643982.7	4699491.0	401.09	-
	un12	2	644240.8	4699753.6	401.09	46,152.96

	un13	7	645100.8	4694078.3	258.78	-
	un28	7	644296.6	4694614.6	350.39	-
Villarluengo	vi14	3	727270.3	4511291.6	286.69	49,447.92
	vi15	2	727036.2	4511166.4	344.58	35,912.14
	vi16	2	727080.8	4511157.8	344.58	47,463.93
	vi17	2	726201.4	4503645.7	520.54	26,659.39
	vi18	2	726118.3	4503470.2	520.54	42,036.27
	vi19	2	726672.8	4503511.0	737.29	17,187.46
	vi20	2	726746.0	4503541.1	737.29	18,689.68
	vi27	7	725543.4	4507042.2	386.36	-
	vi29	2	725332.8	4506874.6	426.13	31,546.16
	vi30	3	725369.2	4506806.6	426.13	43,004.04
	vi36	7	738378.0	4510231.1	425.54	-
	vi37	2	738317.9	4510185.8	425.54	-
	vi38	3	726062.4	4509797.7	570.69	50,681.73
	vi39	3	725818.5	4509536.0	441.26	36,774.11
	vi40	3	725846.4	4509684.0	441.26	32,018.89
	vi41	7	726150.4	4509715.6	570.69	68,006.40
Zuera	zu30	2	674321.2	4636134.8	448.03	47,760.41
	zu31	2	674042.8	4636569.9	458.81	77,218.45
	zu32	5	673137.1	4637107.1	478.08	23,244.28
	zu35	7	671227.6	4642052.5	903.85	-
	zu38*	4	674071.5	4639208.6	822.62	21,633.29
	zu201	4	675701.7	4640029.0	305.40	49,040.58
	zu202	4	675677.7	4640049.3	305.40	85,760.62

* Plot of 10 m circular radius due to terrain constraints.

Table S2. Number of pairs of Prometheus fuel types able to differentiate
(value 1 means Dunn's test, $P \leq 0.05$) by the UAV variables.

Variable	FT2 – FT3	FT2 – FT4	FT2 – FT5	FT2 – FT6	FT2 – FT7	FT3 – FT4	FT3 – FT5	FT3 – FT6	FT3 – FT7	FT4 – FT5	FT4 – FT6	FT4 – FT7	FT5 – FT6	FT5 – FT7	FT6 – FT7	Total pairs
Elev.strata..above.4.00..stddev			1	1	1		1	1	1	1	1	1				9
Elev.CV			1	1	1		1		1	1			1	1		8
Elev.L.kurtosis	1	1		1	1		1			1			1	1		8
Elev.P90			1	1	1		1		1	1	1	1				8
Elev.P95			1	1	1		1		1	1	1	1				8
Elev.P99			1	1	1		1		1	1	1	1				8
Elev.strata..above.4.00..mean			1	1	1		1		1	1	1	1				8
Elev.strata..above.4.00..mode			1	1	1		1	1	1	1		1				8
Elev.strata..above.4.00..median			1	1	1		1		1	1	1	1				8
Elev.maximum			1	1	1		1			1	1	1				7
Elev.stddev			1	1	1			1	1		1	1				7
Elev.variance			1	1	1			1	1		1	1				7
Elev.L2			1	1	1			1	1		1	1				7
Elev.L3			1	1	1		1	1	1	1						7
Elev.L.CV			1		1		1		1	1			1	1		7
Elev.P10			1	1	1		1		1	1			1			7
Elev.P20			1	1	1		1		1	1			1			7
Elev.P40			1	1	1		1	1	1	1						7
Elev.P70			1	1	1		1		1	1		1				7
Elev.P75			1	1	1		1		1	1		1				7
Elev.P80			1	1	1		1		1	1		1				7
Elev.SQRT.mean.SQ			1	1	1		1		1	1		1				7
Elev.CURT.mean.CUBE			1	1	1		1		1	1		1				7
Percentage.all.returns.above.4.00			1	1	1		1			1	1	1				7
All.returns.above.4.00			1	1	1		1			1	1	1				7
Elev.strata..above.4.00..total.returns.count			1	1	1		1			1	1	1				7
Elev.strata..above.4.00..return.proportion			1	1	1		1			1	1	1				7
Elev.strata..above.4.00..max			1	1	1		1			1	1	1				7
Elev.strata..above.4.00..CV			1	1	1			1	1		1	1				7
Elev.mean			1	1	1		1		1	1						6
Elev.kurtosis				1	1		1			1			1	1		6
Elev.AAD				1	1			1	1		1	1				6
Elev.L1			1	1	1		1		1	1						6
Elev.L.skewness			1	1	1		1		1	1						6
Elev.P50			1	1	1		1		1	1						6
Elev.P60			1	1	1		1		1	1						6
Canopy.relief.ratio			1	1	1		1		1	1						6
Percentage.first.returns.above.4.00			1	1	1					1	1	1				6
All.returns.above.4.00.....Total.first.returns.....100			1	1	1					1	1	1				6
First.returns.above.4.00			1	1	1					1	1	1				6
Percentage.all.returns.above.mean			1	1	1		1	1	1							6
All.returns.above.mean			1	1	1		1	1	1							6
Elev.strata..below.0.60..return.proportion			1	1	1		1		1	1						6
Profile.area			1	1	1		1		1	1						6
rumple_general			1	1	1			1			1	1				6
Elev.mode			1				1			1			1	1		5
Elev.IQ				1	1						1	1	1			5
Elev.skewness			1	1	1		1			1						5
Elev.MAD.median			1	1	1						1	1				5
Elev.MAD.mode			1	1	1			1	1							5
Elev.L4			1				1			1			1	1		5
Elev.P01			1	1	1		1		1							5
Elev.P05			1	1	1		1		1							5

[illegible]

Total.first.returns	0														
Total.all.returns	0														
Elev.strata..below.0.60..kurtosis	0														
Elev.strata..0.60.to.2.00..kurtosis	0														
Elev.strata..2.00.to.4.00..kurtosis	0														
Total variables	6	3	12	15	18	1	10	2	3	12	4	1	15	19	0

Table S3. Confusion matrix of the SVM-L classification model of the UAV data.

Fuel types		Predicted						Prod.'s accuracy
		FT2	FT3	FT4	FT5	FT6	FT7	
Actual	FT2	109	20	0	0	0	0	84.50%
	FT3	1	40	0	19	0	1	65.57%
	FT4	0	0	50	0	0	0	100.00%
	FT5	0	0	0	121	0	11	91.67%
	FT6	0	0	0	0	0	0	0.00%
	FT7	0	10	0	0	120	228	63.69%
User's accuracy		99.09%	57.14%	100.00%	86.43%	0.00%	95.00%	

Table S4. F-score (F) coefficient for each fuel type of the SVM-L classification model of the UAV data.

	FT2	FT3	FT4	FT5	FT6	FT7
F	0.91	0.61	1.00	0.89	0.00	0.76

Table S5. Confusion matrix of the SVM-R classification model of the UAV data.

Fuel types		Predicted						Prod.'s accuracy
		FT2	FT3	FT4	FT5	FT6	FT7	
Actual	FT2	101	28	0	0	0	0	78.29%
	FT3	9	32	0	10	0	2	60.38%
	FT4	0	0	41	0	0	2	95.35%
	FT5	0	0	0	118	0	10	92.19%
	FT6	0	0	0	0	97	46	67.83%
	FT7	0	10	9	12	23	180	76.92%
User's accuracy		91.82%	45.71%	82.00%	84.29%	80.83%	75.00%	

Table S6. F-score (F) coefficient for each fuel type of the SVM-R classification model of the UAV data.

	FT2	FT3	FT4	FT5	FT6	FT7
F	0.85	0.52	0.88	0.88	0.74	0.76

Table S7. Confusion matrix of the SVM-L classification model of the UAV-HMLS data.

Fuel types		Predicted						Prod.'s accuracy
		FT2	FT3	FT4	FT5	FT6	FT7	
Actual	FT2	90	10	0	0	0	0	90.00%
	FT3	10	40	10	10	0	1	56.34%
	FT4	0	0	40	0	0	9	81.63%
	FT5	0	0	0	80	0	0	100.00%
	FT6	0	0	0	0	60	18	76.92%
	FT7	0	0	0	0	10	42	80.77%
User's accuracy		90.00%	80.00%	80.00%	88.89%	85.71%	60.00%	

Table S8. F-score (F) coefficient for each fuel type of the SVM-L classification model of the UAV-HMLS data.

	FT2	FT3	FT4	FT5	FT6	FT7
F	0.90	0.66	0.81	0.94	0.81	0.69

Table S9. Confusion matrix of the SVM-R classification model of the UAV-HMLS data.

Fuel types		Predicted						Prod.'s accuracy
		FT2	FT3	FT4	FT5	FT6	FT7	
Actual	FT2	90	10	0	0	0	0	90.00%
	FT3	10	40	9	0	0	2	65.57%
	FT4	0	0	41	0	0	8	83.67%
	FT5	0	0	0	90	0	0	100.00%
	FT6	0	0	0	0	60	9	86.96%
	FT7	0	0	0	0	10	51	83.61%
User's accuracy		90.00%	80.00%	82.00%	100.00%	85.71%	72.86%	

Table S10. F-score (F) coefficient for each fuel type of the SVM-R classification model of the UAV data.

	FT2	FT3	FT4	FT5	FT6	FT7
F	0.90	0.72	0.83	1.00	0.86	0.78

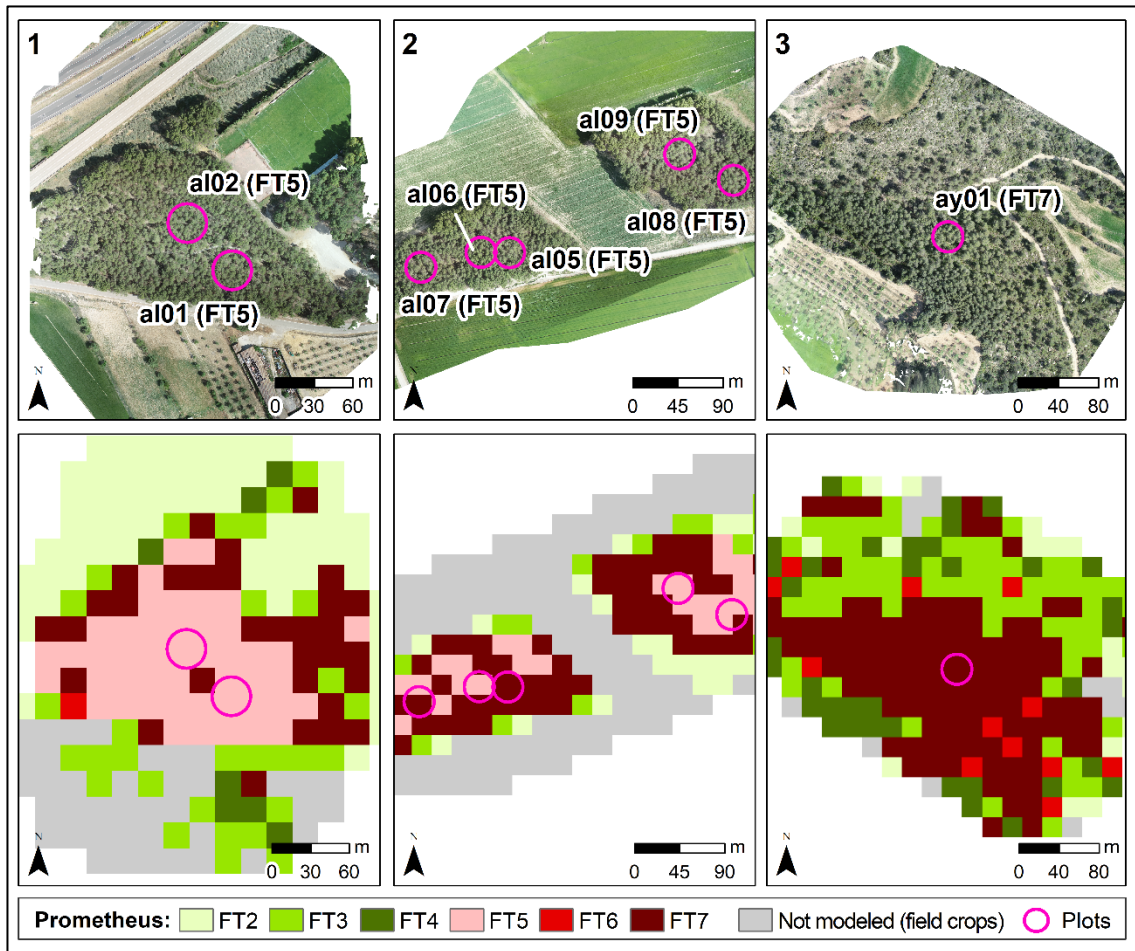


Figure S1. Mapping of Prometheus fuel types from the best classification model (RF) of the UAV data at 20 m spatial resolution. (1) Plots "al01" and "al02". (2) Plots "al05", "al06", "al07", "al08", and "al09". (3) Plot "ay01".

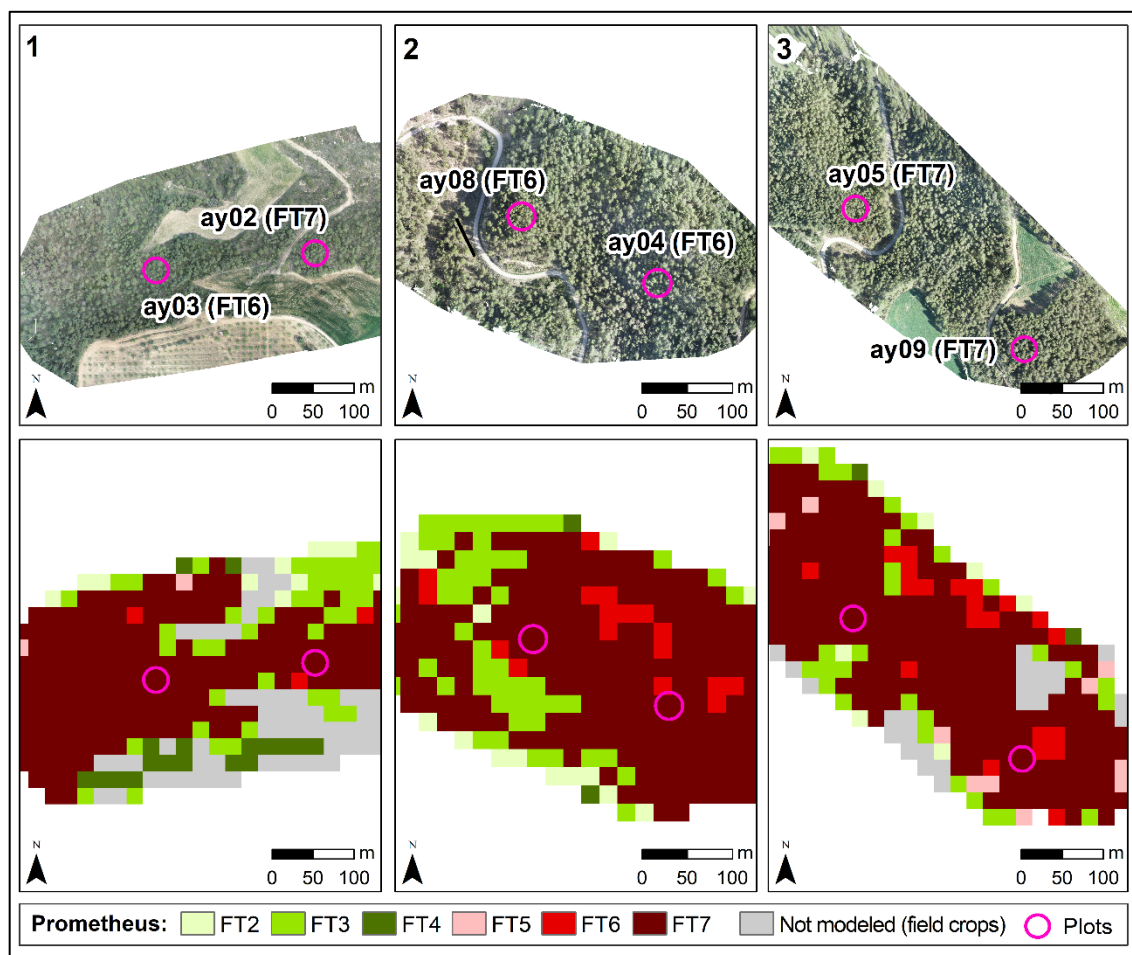


Figure S2. Mapping of Prometheus fuel types from the best classification model (RF) of the UAV data at 20 m spatial resolution. (1) Plots "ay02" and "ay03". (2) Plots "ay04" and "ay08". (3) Plots "ay05" and "ay09".

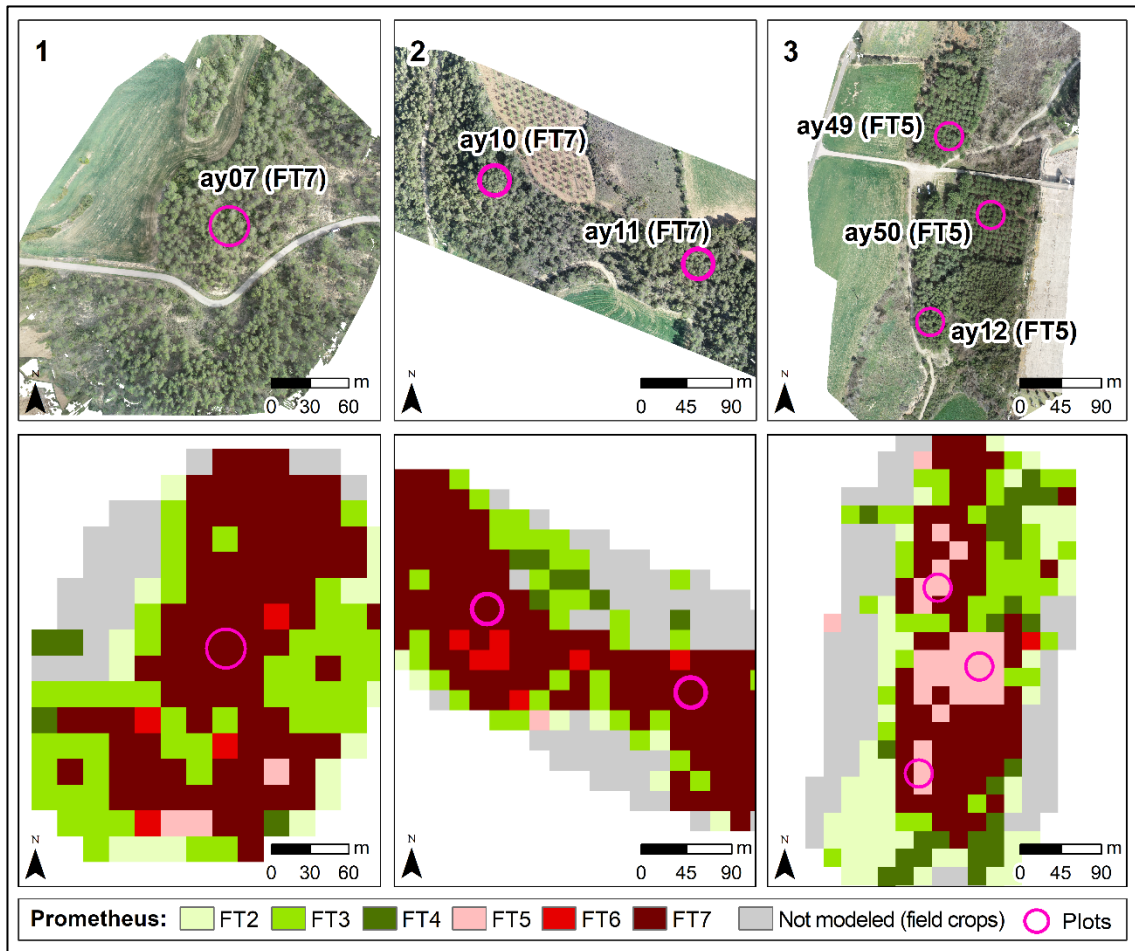


Figure S3. Mapping of Prometheus fuel types from the best classification model (RF) of the UAV data at 20 m spatial resolution. (1) Plot "ay07". (2) Plots "ay10" and "ay11". (3) Plots "ay12", "ay49", and "ay50".

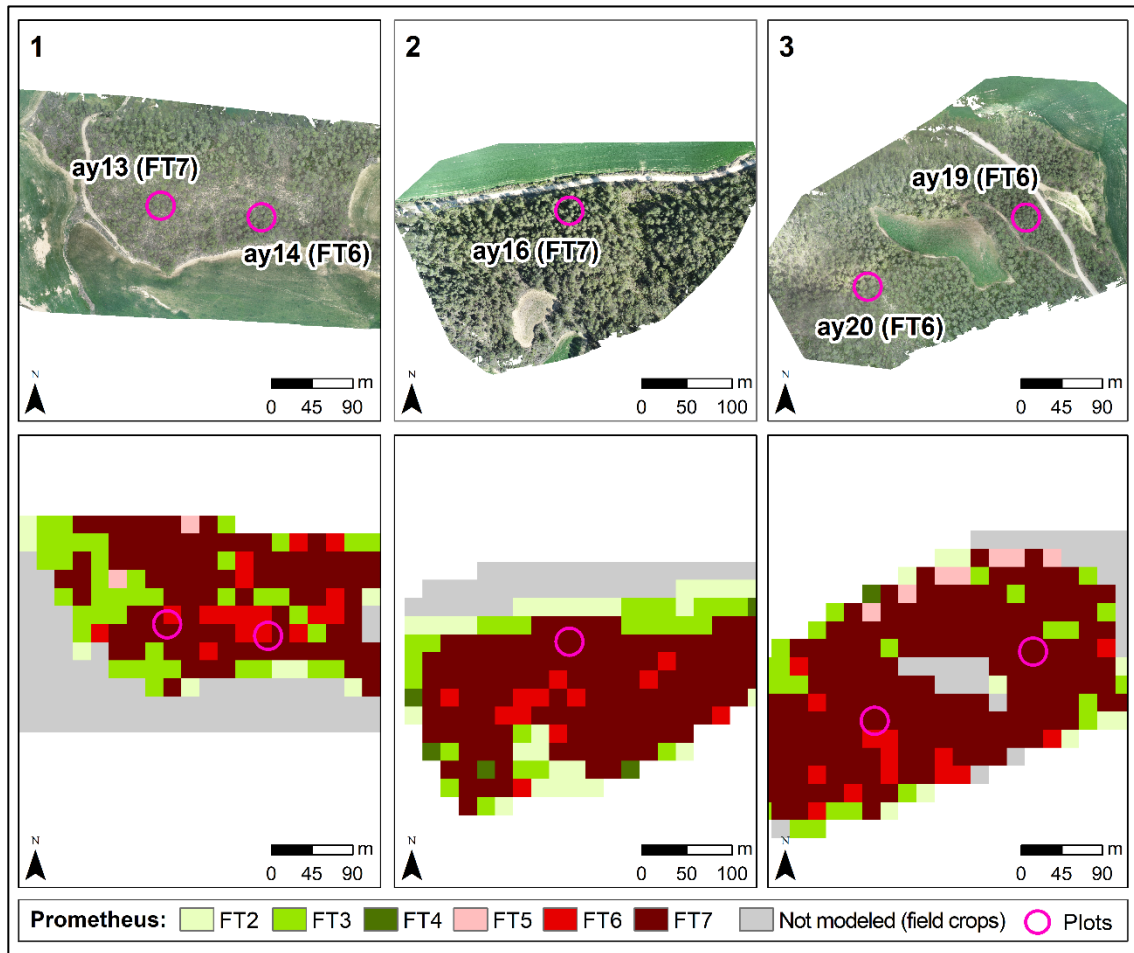


Figure S4. Mapping of Prometheus fuel types from the best classification model (RF) of the UAV data at 20 m spatial resolution. (1) Plots "ay13" and "ay14". (2) Plot "ay16". (3) Plots "ay19" and "ay20".

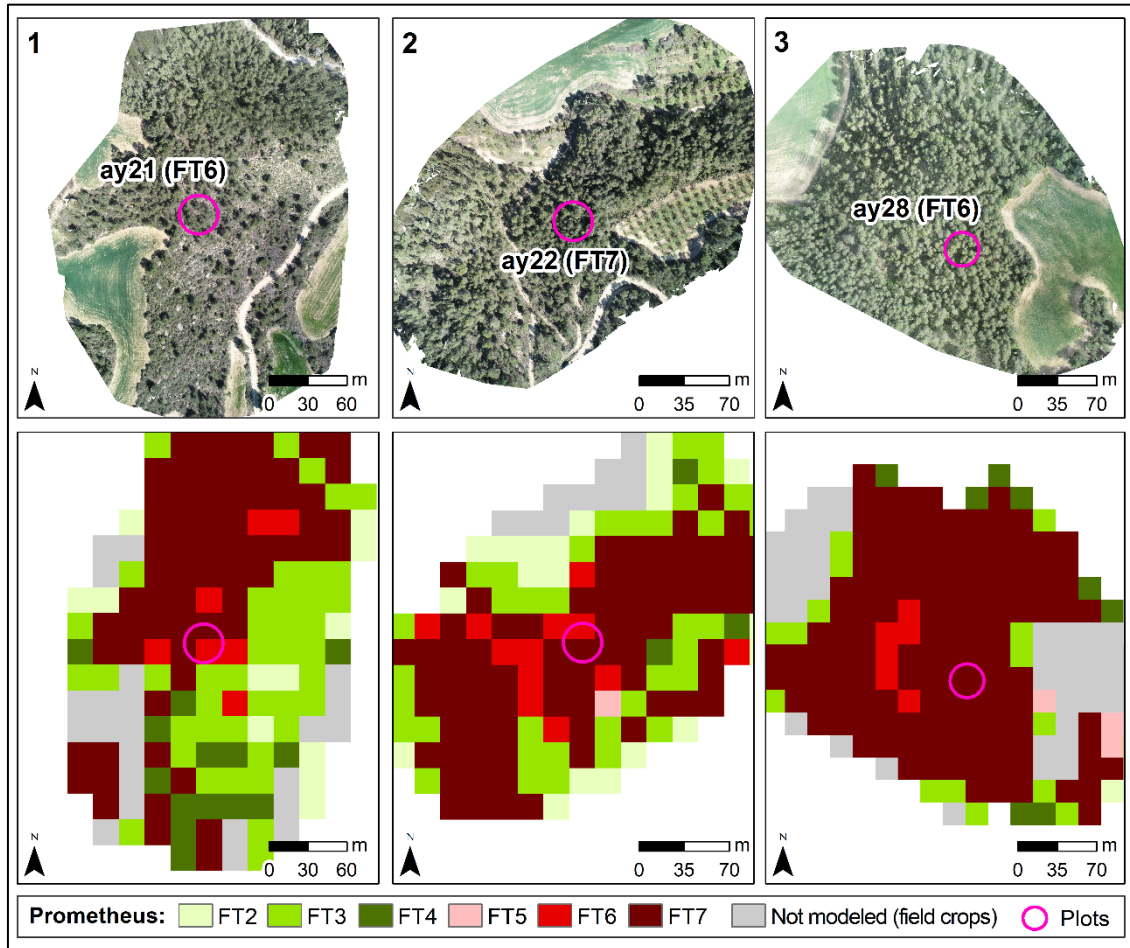


Figure S5. Mapping of Prometheus fuel types from the best classification model (RF) of the UAV data at 20 m spatial resolution. (1) Plot "ay21". (2) Plot "ay22". (3) Plot "ay28".

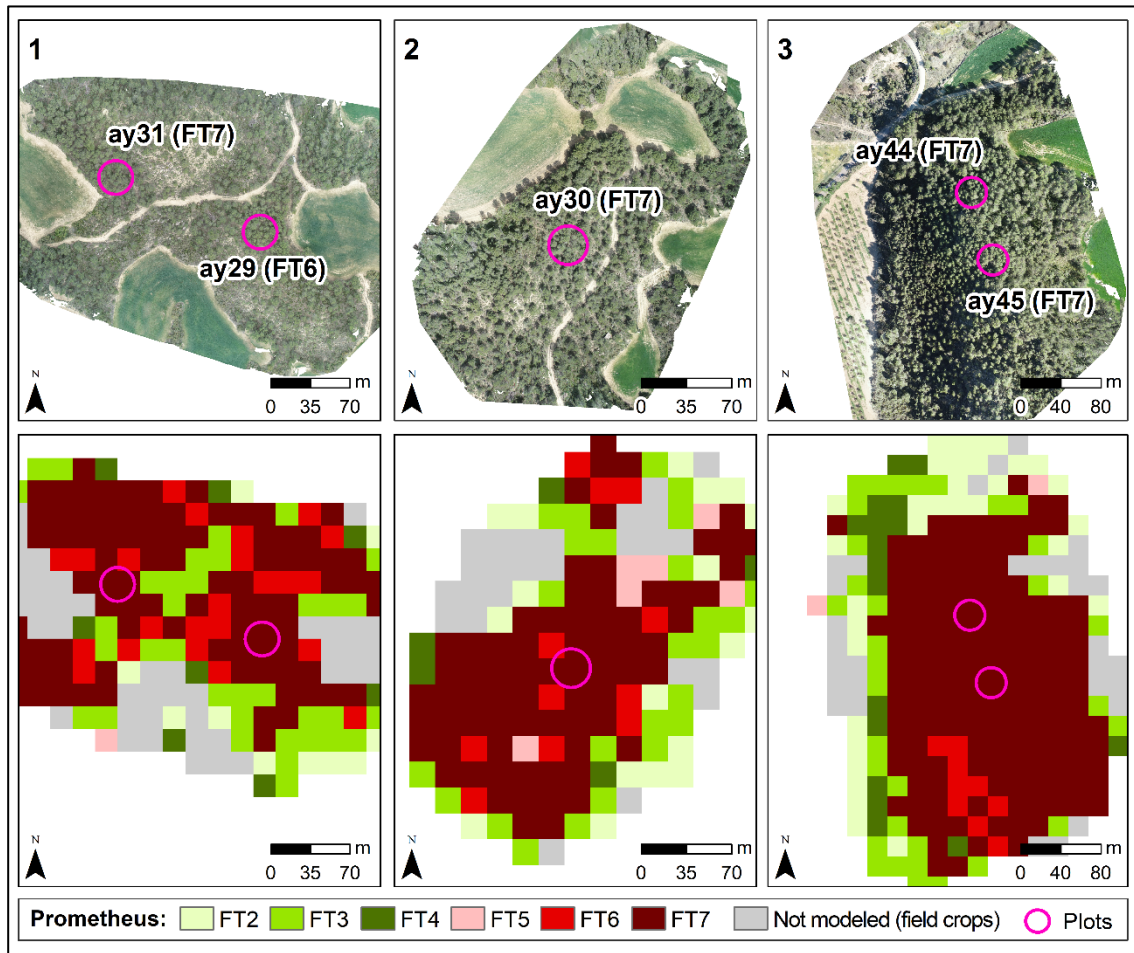


Figure S6. Mapping of Prometheus fuel types from the best classification model (RF) of the UAV data at 20 m spatial resolution. (1) Plots "ay29" and "ay31". (2) Plot "ay30". (3) Plots "ay44" and "ay45".

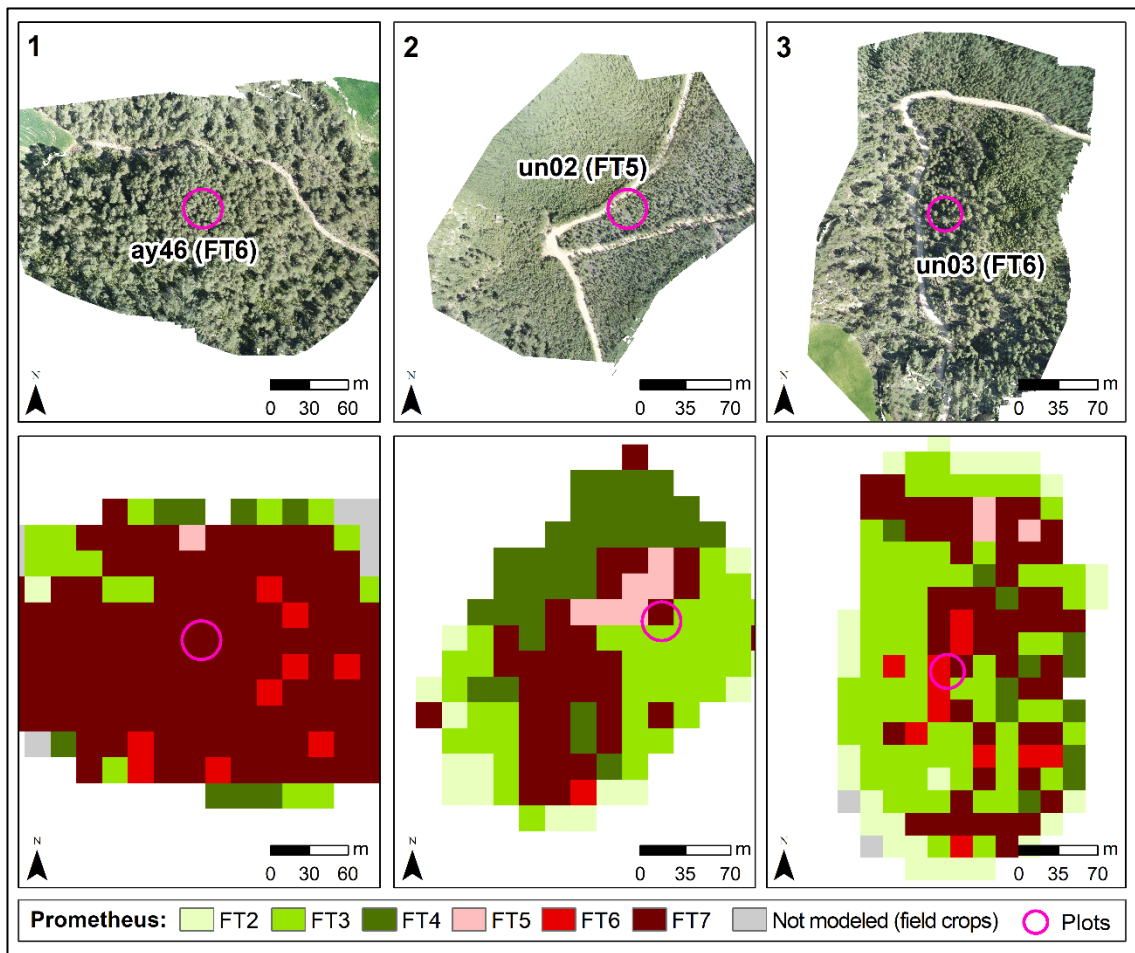


Figure S7. Mapping of Prometheus fuel types from the best classification model (RF) of the UAV data at 20 m spatial resolution. (1) Plot "ay46". (2) Plot "un02". (3) Plot "un03".

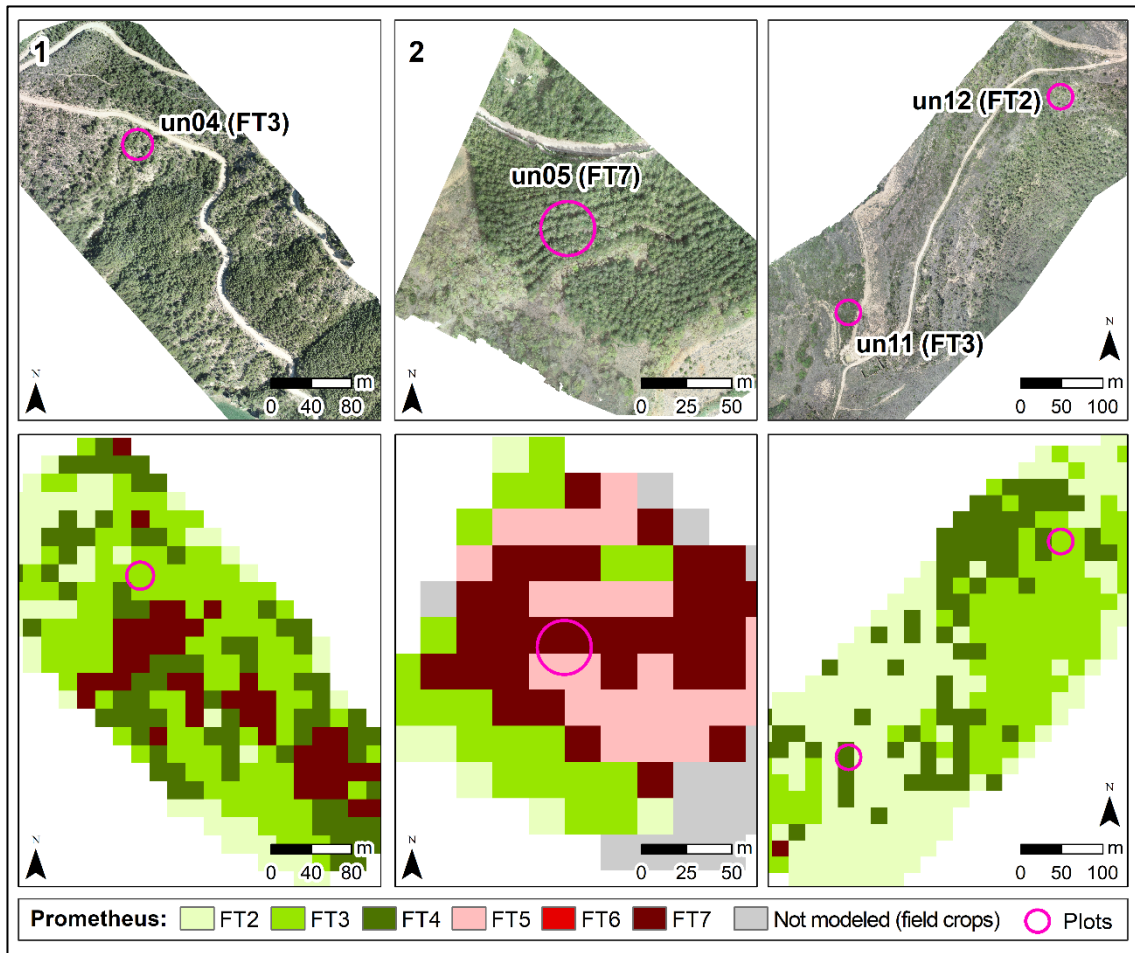


Figure S8. Mapping of Prometheus fuel types from the best classification model (RF) of the UAV data at 20 m spatial resolution. (1) Plot "un04". (2) Plot "un05". (3) Plots "un11" and "un12".

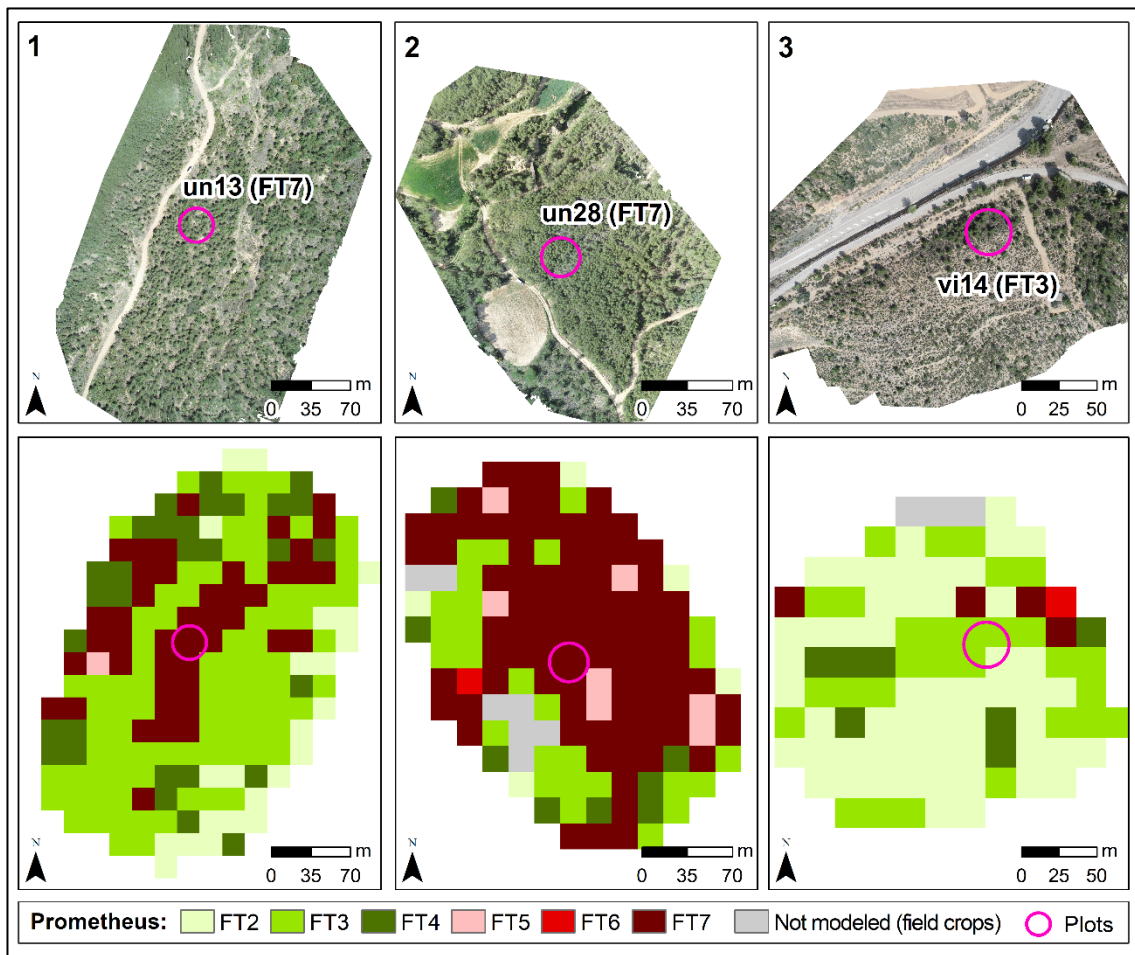


Figure S9. Mapping of Prometheus fuel types from the best classification model (RF) of the UAV data at 20 m spatial resolution. (1) Plot "un13". (2) Plot "un28". (3) Plot "vi14".

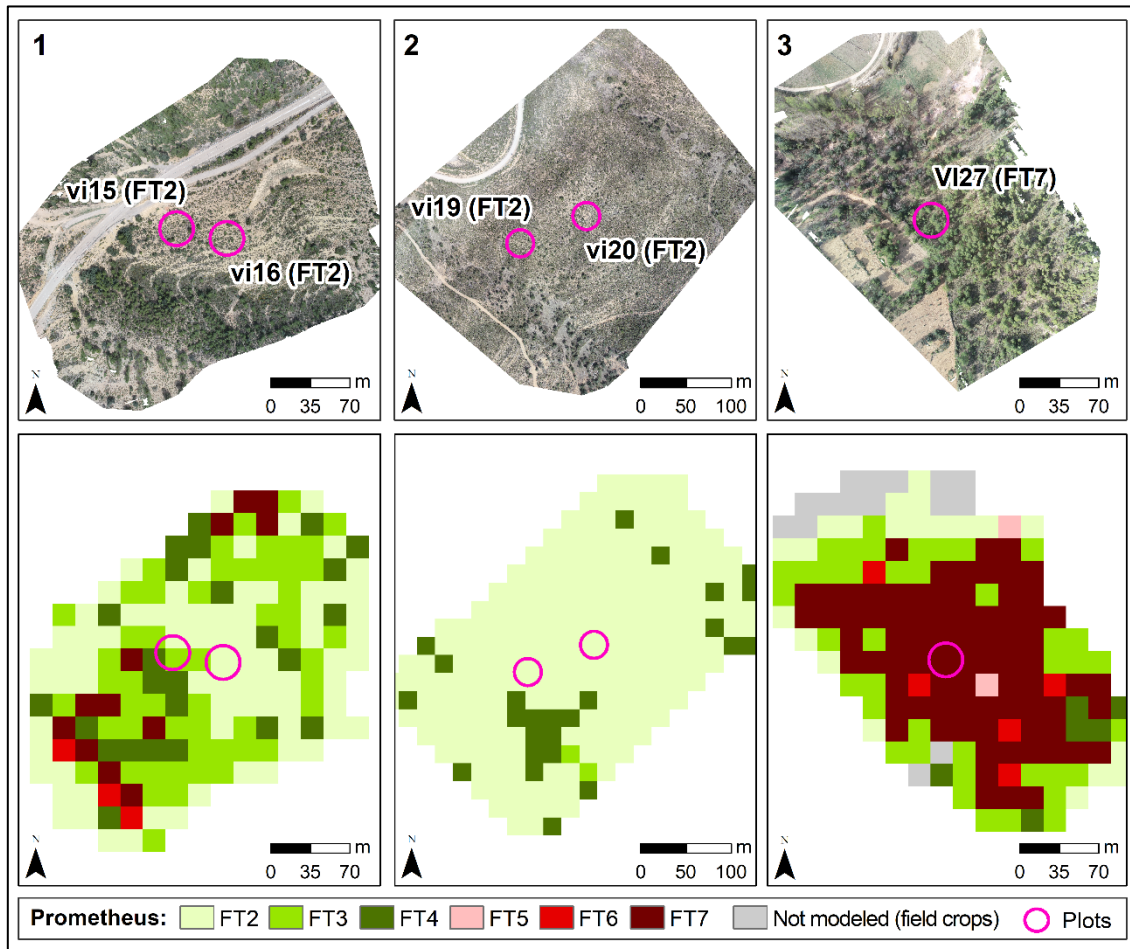


Figure S10. Mapping of Prometheus fuel types from the best classification model (RF) of the UAV data at 20 m spatial resolution. (1) Plots "vi15" and "vi16". (2) Plots "vi19" and "vi20". (3) Plot "vi27".

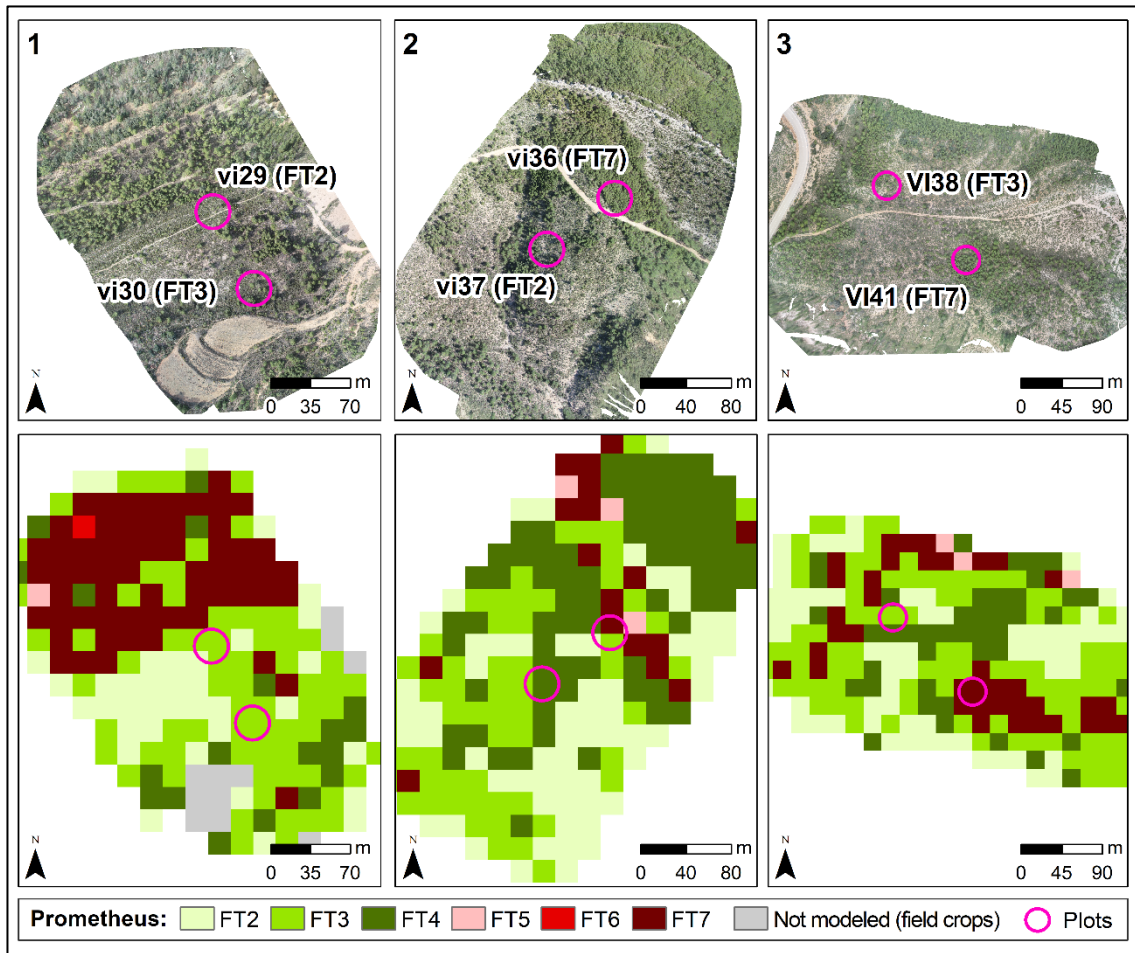


Figure S11. Mapping of Prometheus fuel types from the best classification model (RF) of the UAV data at 20 m spatial resolution. (1) Plots "vi29" and "vi30". (2) Plots "vi36" and "vi37". (3) Plots "vi38" and "vi41".

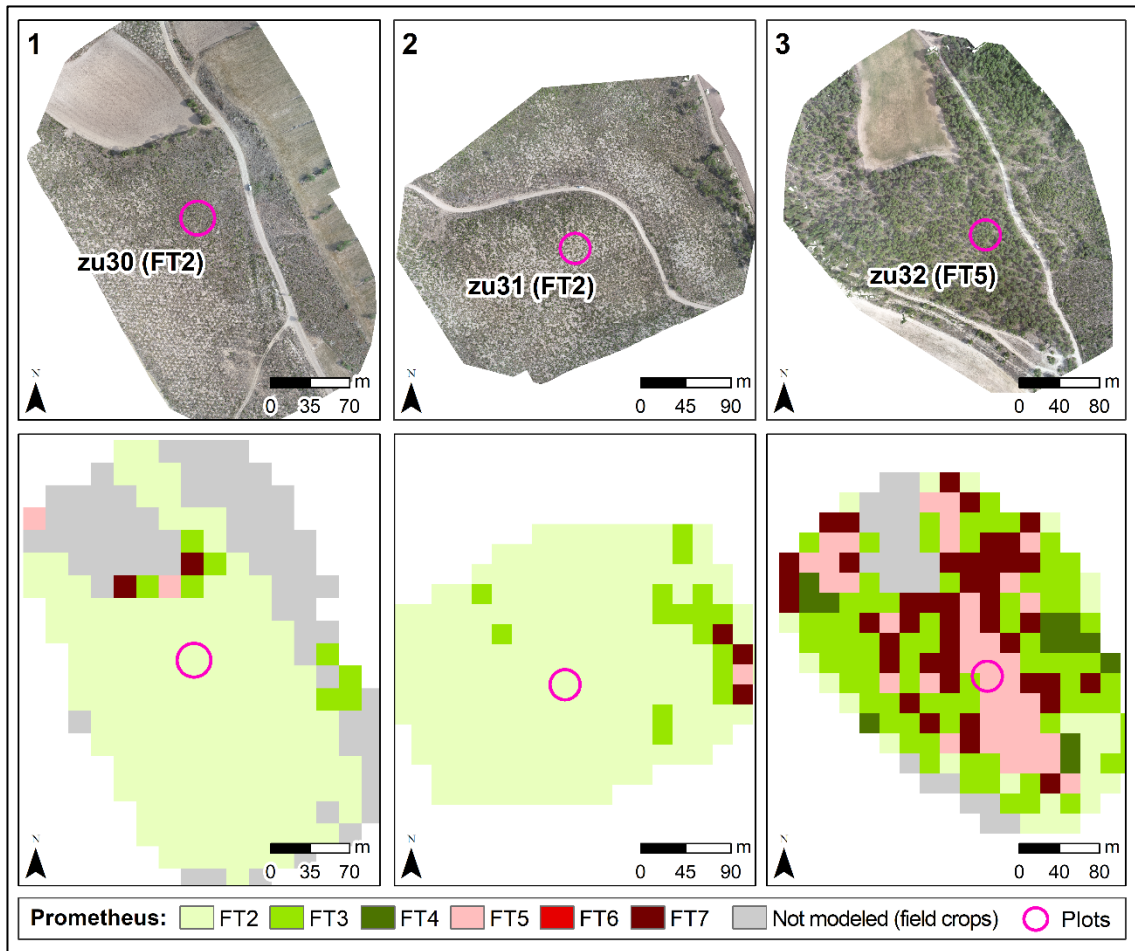


Figure S12. Mapping of Prometheus fuel types from the best classification model (RF) of the UAV data at 20 m spatial resolution. (1) Plot "zu30". (2) Plot "zu31". (3) Plot "zu32".

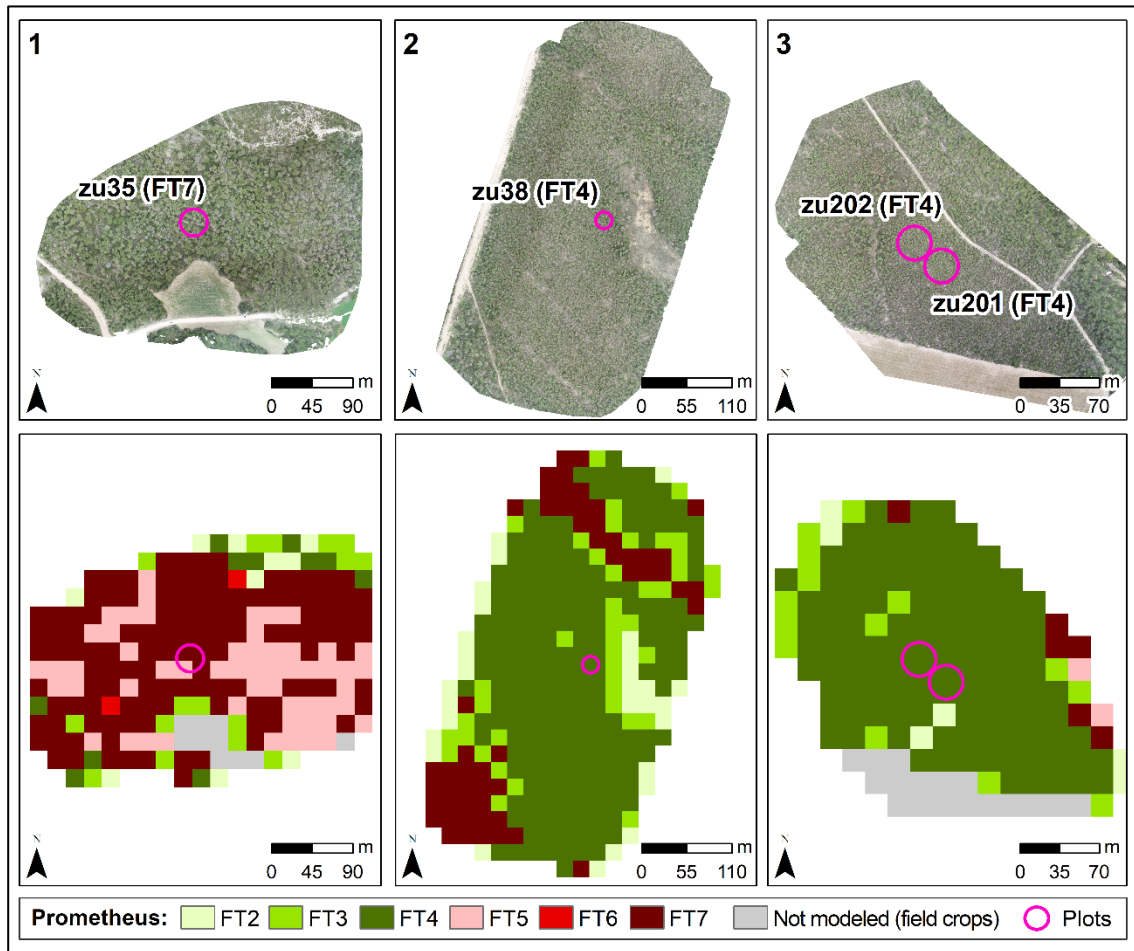


Figure S13. Mapping of Prometheus fuel types from the best classification model (RF) of the UAV data at 20 m spatial resolution. (1) Plot "zu35". (2) Plot "zu38". (3) Plots "zu201" and "zu202".